FABAD J. Pharm. Sci., 51, 3, 1407-1426, 2026
Doi: 10.55262/fabadeczacilik.1990289
RESEARCH ARTICLE

Experimental Screening and Kinetic Characterization of Natural SARS-CoV-2 3CLpro Inhibitors with Cell-Based Antiviral Evaluation

Beyza Tutku BICAKCI[*], Oguz BAYRAKTAR[**], Irem Evfa KUCUK[***], Aylin SENDEMIR[****], Aykut OZKUL[*****], Dilek YALCIN[******°]

Experimental Screening and Kinetic Characterization of Natural SARS-CoV-2 3CLpro Inhibitors with Cell-Based Antiviral Evaluation

SUMMARY

The SARS-CoV-2 main protease (3CLpro) is a key antiviral target essential for viral replication. In this study, a fully experimental screening of a 384-compound natural product library was performed using an optimized FRET-based assay to identify SARS-CoV-2 3CLpro inhibitors. Initial screening identified 57 compounds showing >50% inhibition at 25 μM, from which 24 candidates were selected for dose–response analysis based on inhibitory activity, assay compatibility, predicted toxicity, structural diversity, and literature relevance. Six lead compounds were further characterized through steady-state kinetic analysis, demonstrating competitive, uncompetitive, mixed-type, and possible irreversible inhibition mechanisms, together with Ki determination. To establish their biological relevance, eight selected compounds were subsequently evaluated in Vero E6 cells for cytotoxicity and antiviral activity against the SARS-CoV-2 Omicron variant. RT-qPCR analysis revealed moderate reductions in viral RNA levels, in particular, for Palmitic acid, Vasicine and Anacardic acid at 24 h under non-cytotoxic conditions, supporting a correlation between enzymatic inhibition and antiviral activity. Overall, this study provides a comprehensive experimental dataset for natural SARS-CoV-2 3CLpro inhibitors and highlights promising hit compounds for future antiviral development.

Keywords: *SARS-CoV-2, proteases, natural compounds, inhibitors, experimental screening*

Doğal Bileşik Kaynaklı SARS-CoV-2 3CLpro İnhibitörlerinin Deneysel Taraması, Kinetik Karakterizasyonu ve Hücre Bazlı Antiviral Etkilerinin İncelenmesi

ÖZ

SARS-CoV-2 ana proteazı (3CLpro), viral replikasyon için gerekli olan temel bir enzim olup antiviral tedaviler açısından önemli bir hedef olarak kabul edilmektedir. Bu çalışmada, SARS-CoV-2 3CLpro inhibitörlerini belirlemek amacıyla 384 doğal bileşikten oluşan bir kütüphane, optimize edilmiş FRET (Floresans Rezonans Enerji Transferi) temelli bir yöntem kullanılarak tamamen deneysel olarak taranmıştır. İlk taramada 25 μM konsantrasyonda %50'nin üzerinde inhibisyon gösteren elli yedi bileşik arasından yirmi dört bileşik, inhibisyon aktiviteleri, tayin yöntemiyle uyumluluk, tahmini toksisite, yapısal çeşitlilik ve literatüre yakınlık gibi kriterler göz önünde bulundurularak üzerinde doz-yanıt analizlerini gerçekleştirmek üzere seçilmiştir. En güçlü altı aday bileşik, kararlı durum enzim kinetiği analizleri ile ayrıntılı olarak incelenmiş; kompetitif, unkompetitif, karışık tip ve olası geri dönüşümsüz inhibisyon mekanizmaları ortaya konulmuş ve Ki değerleri belirlenmiştir. Biyolojik etkinliklerinin değerlendirilmesi amacıyla seçilen sekiz bileşik, Vero E6 hücrelerinde sitotoksisite ve SARS-CoV-2 Omicron varyantına karşı antiviral aktiviteleri açısından test edilmiştir. RT-qPCR analizleri, sitotoksik olmayan konsantrasyonlarda özellikle Palmitik asit, Vasisin ve Anakardik asit'in 24 saatte viral RNA düzeylerinde orta düzeyde azalma sağladığını göstermiş ve enzim inhibisyonu ile antiviral aktivite arasında bir ilişki bulunduğunu desteklemiştir. Sonuç olarak bu çalışma, doğal kaynaklı SARS-CoV-2 3CLpro inhibitörlerine ilişkin kapsamlı bir deneysel veri seti sunmakta ve gelecekteki antiviral ilaç geliştirme çalışmaları için umut vadeden aday bileşikleri ortaya koymaktadır.

Anahtar Kelimeler: *SARS-CoV-2, proteazlar, doğal bileşikler, inhibitörler, deneysel tarama*

Recieved: 08.07.2026
Revised: 05.10.2026
Accepted: 14.10.2026

* ORCID: 0000-0002-6638-0355, Department of Bioengineering, Ege University, Bornova, Izmir, 35100, Türkiye
** ORCID: 0000-0003-4210-2825, Department of Bioengineering, Ege University, Bornova, Izmir, 35100, Türkiye
*** ORCID: 0009-0005-2168-0951, Department of Bioengineering, Ege University, Bornova, Izmir, 35100, Türkiye
**** ORCID: 0000-0003-1818-6651, Department of Bioengineering, Ege University, Bornova, Izmir, 35100, Türkiye
***** ORCID: 0000-0001-5008-9443, Department of Virology, Faculty of Veterinary Medicine Ankara University, Ankara, 06070, Türkiye
****** ORCID: 0009-0002-5243-7434, Department of Bioengineering, Izmir Institute of Technology, Urla, Izmir, 35430, Türkiye

° Corresponding Author; Dilek Yalcin
E-mail: dilekyalcin@iyte.edu.tr

INTRODUCTION

SARS-CoV-2, which emerged in December 2019 in Wuhan, China, has caused over 7 million deaths worldwide and triggered urgent efforts to develop vaccines and antiviral therapeutics (WHO, 2026; Yadav et al., 2021). This positive-sense RNA *Betacoronavirus* encodes structural proteins (S, E, M, N) and two polyproteins (pp1a/pp1ab), which are cleaved by viral proteases PLpro and 3CLpro into non-structural proteins required for replication (Malone, Urakova, Snijder, & Campbell, 2022). Among these enzymes, 3CLpro is essential because it processes viral polyproteins at 11 conserved sites and suppresses host antiviral responses by modulating interferon and NF-κB signaling (Shen et al., 2022). Structurally, 3CLpro functions as a homodimer with a catalytic dyad (Cys145–His41) located between domains I and II and exhibits high substrate specificity for Leu-Gln↓ (Ser, Ala, Gly) motifs, unlike any human protease. Its early role in the viral life cycle, unique structure, and lack of human homolog make 3CLpro an attractive target for broad-spectrum antiviral drug development (Ghosh, Chakraborty, Biswas, & Chowdhuri, 2021; Kuzikov et al., 2021).

Natural compounds have emerged as a valuable yet underexplored resource in the ongoing search for effective SARS-CoV-2 therapeutics due to their structural diversity, broad bioactivity, and potential to overcome limitations of conventional antivirals against emerging variants (Bahun et al., 2022). Their complex architectures allow them to modulate multiple biological pathways and target various stages of the viral life cycle or key viral and host proteins (Isidoro, Chiung-Fang Chang, & Sheen, 2022; Szabó, Crowe, Mamotte, & Strappe, 2024). This chemical diversity, spanning alkaloids, flavonoids, terpenoids, and peptides, supports high-affinity interactions that are often difficult to achieve with synthetic molecules, while many natural products also possess favorable pharmacological properties (Atanasov et al., 2021).

Since the onset of the pandemic, a number of *in vitro* studies have investigated natural products and drug-like molecules as potential inhibitors of the SARS-CoV-2 3CLpro enzyme. Coelho et al. (2020) screened 2,400 approved drugs and natural compounds using a FRET-based assay and identified 13 inhibitors with IC_{50} values between 0.2 μM and 23 μM (Coelho, Gallo, Campos, Hardy, & Wurtele, 2020). Bahun et al. examined 19 polyphenols and reported that quercetin, ellagic acid, curcumin, EGCG, and resveratrol achieved over 50% inhibition at 10 μM, with corresponding IC_{50} values ranging from 11.8 μM to 23.4 μM (Bahun et al., 2022). Other studies broadened this landscape: Glaab et al. (2021) combined machine learning and *in silico* molecular docking to evaluate over 95 molecules; Zhu et al. (2020) identified 23 inhibitors through biochemical assays; and Krüger et al. (2023) assessed 31 natural and synthetic compounds using IC_{50} profiling (Glaab, Manoharan, & Abankwa, 2021; Krüger et al., 2023; Zhu et al., 2020). Likewise, galloylated polyphenols such as epigallocatechin gallate (0.40 μM) and theaflavin-3,3′-digallate (7.80 μM) exhibited superior inhibition compared with their non-galloylated counterparts (Hariono et al., 2021). A recent study evaluated several natural compounds isolated from *Bletilla striata,* including baicalin, gastrodin, physcion, caffeic acid, 3'-O-methyl dioscin III, blestritin B, gymconopin D, and pleiobibenzynin B, for their ability to inhibit SARS-CoV-2 3CLpro using a FRET-based assay, reporting IC_{50} values between 0.98 μM and 39 μM (Yang et al., 2024). Despite growing interest in natural and synthetic 3CLpro inhibitors, major gaps persist because *in vitro* screening of large compound sets remains costly and labor-intensive. Consequently, most studies rely heavily on large-scale virtual screening, even though computational predictions frequently show poor agreement with biochemical assay results. This limitation has been repeatedly noted in several studies demonstrating weak *in silico*/*in vitro* correlations (Khamto et al., 2025; Zong et al., 2024).

To address these limitations, a comprehensive experimental workflow for the discovery and validation of natural SARS-CoV-2 3CLpro inhibitors was established in this study. A library of 384 natural compounds was systematically screened using an optimized FRET-based enzymatic assay, followed by dose–response analysis, detailed steady-state kinetic characterization, and cell-based antiviral validation of selected hit compounds. Unlike previous studies that relied predominantly on virtual screening or were limited to IC_{50} determination, this work integrates enzymatic screening, inhibition mechanism analysis, K_i determination, cytotoxicity evaluation, and antiviral assessment within a single experimental platform. By generating these experimentally validated datasets for natural 3CLpro inhibitors, this study provides both valuable lead compounds and a comprehensive biochemical resource to support future antiviral drug discovery and rational inhibitor development.

MATERIALS AND METHODS

Materials

The 3CLpro of SARS-CoV-2 with an N-terminal MBP-tag and a sensitive internally quenched fluorogenic substrate were obtained from BPS Bioscience (San Diego, CA, USA). The enzyme, expressed in an *Escherichia coli* expression system, has a molecular weight of 77.5 kDa and was used directly in the assay without cleavage of the MBP tag (Cat No: 100707). The peptide substrate consists of a 14-amino acid sequence (KTSAVLQSGFRKME) with Dabcyl and Edans attached to its N- and C-termini, respectively (Cat No: 79952-1). All natural compounds, sourced from Selleck Chemicals (Houston, TX, USA), are listed with their catalogue numbers in the Natural Product Library (https://www.selleckchem.com/screening/natural-product-library.html), and the full list of compounds used in this study is provided in Table S1. GC376, a well-known 3CLpro inhibitor supplied with the assay kit by the manufacturer (BPS Bioscience, Cat No: 79955), was used as the positive control. Other chemicals included (tris[hydroxmethyl]aminomethane) (Sigma-Aldrich, USA, Cat No: T-1503), EDTA (Amresco, USA, Cat No: 0322), and Dithiothreitol (DTT) (Sigma-Aldrich, US, Cat No: 3483-12-3). In cytotoxicity and virus-infected cell studies, Vero cell lines (ATCC no: CRL-1586) were used as described below.

Determination of steady-state kinetic parameters for SARS-CoV-2 3CLpro

The enzymatic activity and kinetic parameters of SARS-CoV-2 3CLpro were measured using a fluorescence resonance energy transfer (FRET) assay, which monitors substrate cleavage in real time through changes in fluorescence. Assays were performed in black 96-well plates (Greiner Bio-One, Monroe, NC, USA) using the fluorogenic peptide substrate Dabcyl-KTSAVLQSGFRKME-Edans and recombinant 3CLpro. Since the fluorogenic substrate has a very low aqueous solubility, substrate dilutions were made using DMSO. The effect of DMSO concentration on enzyme activity was first evaluated experimentally, and the corresponding results are presented in Figure S1 in the SI. Substrate and enzyme concentrations were then optimized to ensure strong signal sensitivity and efficient reaction performance.

Steady-state kinetics were determined using 50 nM 3CLpro and varying substrate concentrations (5–100 μM). Enzyme concentration optimization was similarly performed using 25 μM substrate and 10–100 nM enzyme. The reactions were initiated by sequentially adding 20 μL of assay buffer (20 mM Tris, 150 mM NaCl, 1 mM EDTA, 1 mM DTT, pH 7.3), 20 μL of substrate solutions, and 60 μL of enzyme solutions, and were incubated at 37 °C for 5 minutes prior to measurement. Using a Thermo Fisher microplate reader, fluorescence was recorded for 2 hours at 5-minute intervals at excitation and emission wavelengths of 355 nm and 460 nm, respectively (Zhu et al., 2020). Initial velocities (V_0) were obtained from the linear region of the fluorescence curves, and kinetic parameters (K_m, V_{max}) were calculated by fitting data to the Michaelis–Menten model using GraphPad Prism 8 software.

Screening of a natural compound library against SARS-CoV-2 3CLpro

Natural compounds were supplied by the vendor as 10 mM stock solutions pre-dissolved in DMSO. Prior to the assay, these stock solutions were further diluted in assay buffer (20 mM Tris, 150 mM NaCl, 1 mM EDTA, 1 mM DTT, pH 7.3) to obtain a final concentration of 25 μM for each compound. In the initial screening assay, each well contained 50 nM 3CLpro, 25 μM FRET substrate (at their optimized concentrations), and 25 μM compound in a total volume of 70 μL. Enzyme–substrate controls were prepared by replacing the compound with 14 μL of buffer. Fluorescence signals were recorded for 2 hours at 37 °C, with excitation and emission wavelengths of 355 nm and 460 nm, respectively. Measurements were taken every 5 minutes. All reactions were duplicated. To calculate percent inhibition, the initial velocity for each well was determined by linear regression of the first linear phase of the kinetic data (RFU vs. time), which was within the first 60 minutes. Percent inhibition was then calculated using the following equation:

$$\% \, Inhibition = \left(1 - \frac{v_0^{compound}}{v_0^{control}}\right) \times 100$$

where $v_0^{compound}$ is the initial velocity in the presence of inhibitor and $v_0^{control}$ is the initial velocity of the control (no inhibitor). Prior to performing the screening study, GC376, a known 3CLpro inhibitor, was used to evaluate and optimize the reliability of the FRET assay under the optimized enzyme and substrate concentrations of 50 nM and 25 μM, respectively. The resulting dose-response curve obtained for GC376 is provided in Figure S2 in the SI.

Complementary toxicity prediction for compound selection

Toxicity profiles of the selected compounds were predicted using the ProTox-III web platform (https://tox.charite.de/protox3/), which employs a machine learning-based approach to estimate various toxicity endpoints such as oral lethal doses, LD_{50} (in mg/kg), Globally Harmonized System (GHS) toxicity class (I–VI), and risks of hepatotoxicity, carcinogenicity, immunotoxicity, mutagenicity, and cytotoxicity. The chemical structures of the compounds were uploaded in SMILES format, and predictions were generated based on molecular similarity, fragment analysis, and known toxicophores. ProTox-III predictions were used as a complementary prioritization tool rather than as an absolute exclusion criterion based on a single predefined toxicity threshold. Predicted LD50 values and GHS toxicity classes were considered together with experimentally measured 3CLpro inhibition (Table S2 in the SI). When compounds showed comparable inhibitory activity, candidates with more favorable predicted toxicity profiles were preferentially prioritized for subsequent characterization.

Determination of half-maximal inhibitory concentrations (IC_{50}) for potential 3CLpro inhibitors

The selected compounds were tested at seven different concentrations (0.1, 0.5, 1, 5, 10, 50, and 100 μM), using fixed 3CLpro enzyme and substrate concentrations (50 nM and 25 μM, respectively). All reactions were carried out in black 96-well microplates at 37 °C as described above. IC_{50} values were determined using nonlinear regression analysis of dose–response curves generated in GraphPad Prism software. All experiments were conducted in duplicate to ensure reproducibility.

Determination of inhibition mechanisms and K_i values for selected SARS-CoV-2 3CLpro inhibitors

Based on IC_{50} values, the most potent inhibitors were selected for detailed kinetic analysis to characterize their binding behavior and inhibition mechanisms. Enzyme inhibition kinetics were investigated using varying substrate concentrations (25, 50, 75, and 100 μM) at a fixed enzyme concentration of 100 nM. Each compound was tested at four different concentrations, determined based on their IC_{50} profiles; Vasicine and Palmitic Acid (1, 5, 10, and 50 μM), Anacardic Acid and Ginkgolic Acid (5, 10, 25, and 50 μM), Neobavaisoflavone and Fisetin (5, 25, 50, and 100 μM), Rutin (25, 50,

100, and 200 µM), and Neochlorogenic Acid, Chlorogenic Acid, Nobiletin, and Naringenin (10, 25, 50, and 100 µM). Assays were performed at 37 °C as described above. Kinetic parameters (V_{max}, K_m, and K_i) in the absence and presence of the inhibitors were determined through nonlinear regression using GraphPad Prism.

Cell culture and cell viability assays

The evaluation of cellular toxicity was conducted employing Vero E6 cells (African green monkey kidney epithelial cells), as per the guidelines stipulated in ISO 10993-5. The cells were cultivated in Dulbecco's Modified Eagle Medium (DMEM; Merck, Lot: F0415), which was enriched with 10% fetal bovine serum (Gibco, Lot: C1642), 1% L-glutamine (Merck, Lot: 1238E), and 1% gentamicin (Merck, Lot: A2712). The experiments involved the seeding of Vero E6 cells at a density of 1×10^5 cells/mL into 96-well plates, with four replicates for each condition. The plates were then incubated at 37 °C with 5% CO_2 for a period of 24 hours. After incubation, the medium was removed, and the cells were treated with the eight selected compounds at concentrations of 25 µM, 12.5 µM, 6.25 µM, 3.125 µM, 1.5625 µM, and 0.78 µM and incubated for an additional 24 or 48 hours, while untreated cells in fresh DMEM served as the negative control. Cell viability was assessed using the MTT (3-(4 5-dimethylthiazol-2-yl)-2 5-diphenyltetrazolium bromide) assay by adding 10% (v/v) MTT solution followed by a 3 h incubation. The resulting formazan crystals were dissolved in DMSO, and absorbance was measured at 570 nm with a 690 nm reference wavelength using a microplate reader. Data are presented as mean ± SD and were analyzed by one-way ANOVA with Bonferroni's post hoc test. Compounds reducing cell viability to ≤70% of the control were classified as cytotoxic, and this threshold is indicated in the graphs.

Cell-based antiviral assay

The 10 mM stock solutions of each compound were diluted 1:1000 in DMEM to create the initial working dilution of 10 µM. The following two-fold dilutions (5 µM, 2.5 µM, and 1.25 µM) were then prepared from this initial step onwards, resulting in four-step dilutions of the compounds. These dilutions were then transferred (100 µL) to Vero E6 cells that had been infected with the SARS-CoV-2 Omicron variant at a multiplicity of infection (MOI) of 0.1 two hours prior. Four replicates were used for each dilution value of each agent for this purpose. The same protocol was performed on two separate plates for incubations lasting 24 and 72 hours. At 24 and 72 hours after treatment, we first examined the cells microscopically to investigate the presence of SARS-CoV-2-specific CPE as a qualitative indicator of virus-induced cellular damage. After recording the CPE findings, the plates were frozen at -80 °C to determine the amount of virus in the compound treated wells in comparison to untreated virus control wells. After thawing the frozen plates at room temperature, 200 µL of the contents from four replicate wells with the most concentrated dilutions of each sample were transferred to separate tubes. Total RNA was then isolated using Trizol LS. A one-step RT-qPCR protocol for GAPDH (housekeeping gene) and N protein coding region of SARS-CoV-2 genomic RNA was also applied to each sample to quantitatively evaluate the antiviral activity. Briefly, each reaction was carried out in a single-tube format using a commercially available one-step RT-qPCR master mix containing SYBR Green I dye, with primers specific to each target. Amplification and fluorescence detection were performed on a Rotor-Gene Q instrument (Qiagen, USA). Melt curve analysis was conducted at the end of each run to confirm amplicon specificity by verifying single-peak dissociation profiles. Relative quantification was performed using the 2^−ΔΔCt method, whereby Ct values for the SARS-CoV-2 N protein target were first normalized to the GAPDH housekeeping gene (ΔCt), and fold-change in viral RNA abundance was subsequently calculated relative to a designated reference sample (ΔΔCt). Results are expressed as fold-change values, with higher values reflecting greater relative viral RNA levels. Fold changes in RNA relative to the virus control were analyzed separately for 24 and 72 hours using two-way ANOVA.

RESULTS AND DISCUSSION

Optimization of enzyme and substrate concentrations for 3CLpro assay

During assay development, the influence of DMSO concentration on enzyme activity was first evaluated because the fluorogenic substrate has a limited aqueous solubility and was prepared in DMSO. High DMSO fractions (e.g. 40% v/v, Figure S1.) were found to significantly reduce enzymatic activity, consistent with previous reports describing solvent-induced enzyme destabilization at elevated DMSO levels (Ferreira et al., 2021; Nguyen et al., 2021). Therefore, subsequent experiments were performed under conditions where the final DMSO concentration did not exceed 20% (v/v).

To establish a reliable FRET-based assay for evaluating SARS-CoV-2 3CLpro activity, optimization experiments were then performed to identify appropriate enzyme and substrate concentrations. For this reason, various enzyme concentrations were initially evaluated using a fixed substrate concentration of 25 μM, as shown in Figure 1a. An enzyme concentration of 50 nM was selected as the optimal condition for subsequent experiments, as it provided a robust and reproducible increase in fluorescence signal within the linear range of the assay. This concentration ensured sufficient enzymatic activity without causing substrate saturation and was consistent with values commonly used in FRET-based 3CLpro assays (Bahun et al., 2022; Kuzikov et al.,2021; Zhu et al., 2020). Maintaining this enzyme concentration also enabled reliable assessment of inhibitor potency while preserving assay sensitivity for the screening. Enzyme kinetics were subsequently analyzed using a fixed 3CLpro concentration (50 nM) and varying substrate concentrations, as shown in Figure 1b. The resulting kinetic parameters, K_m and V_{max}, were obtained by fitting the data to the Michaelis–Menten model, presented in Figure 1c and 1d.

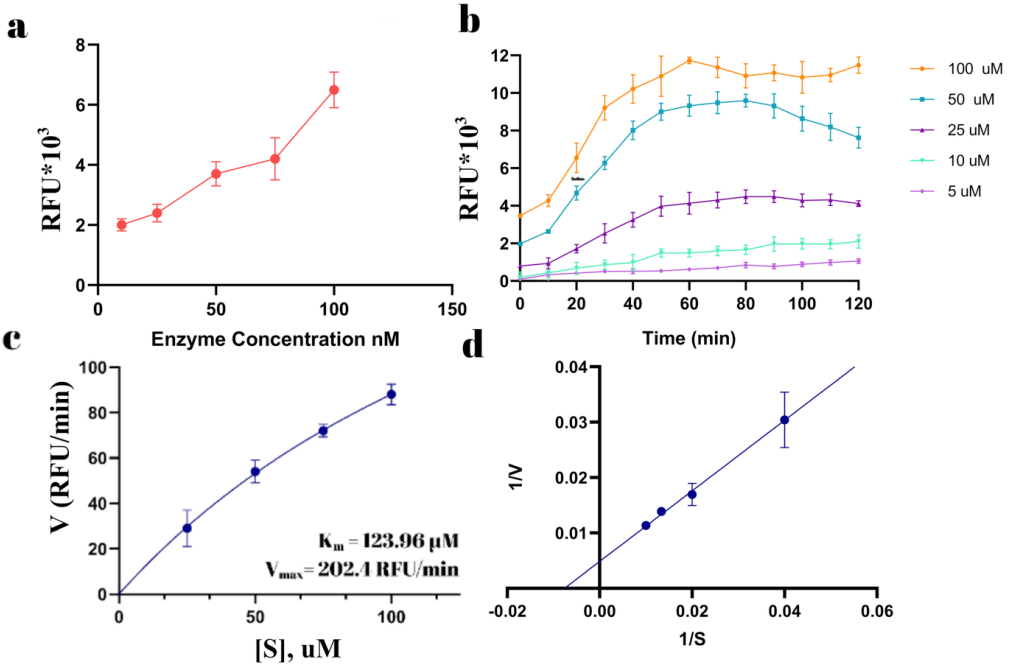

Figure 1. Determination of key enzymatic parameters for SARS-CoV-2 3CLpro (a) change in fluorescence over a 2-hour period for enzyme concentrations ranging from 10 nM to 100 nM at a fixed substrate concentration of 25 μM, (b) change in fluorescence over time for substrate concentrations ranging from 5 μM to 100 μM at a fixed enzyme concentration of 50 nM, (c, d) Michaelis-Menten and Lineweaver-Burk plots obtained at 50 nM 3CLpro and 25 μM substrate concentrations, respectively.

Based on the results shown in Figure 1a and 1b, substrate and enzyme concentrations of 25 μM and 50 nM, respectively, were selected as the optimal conditions for the FRET-based assay. Kinetic analysis using GraphPad yielded a Km of 123.96 μM and a Vmax of 202.4 RFU/min. Since the substrate concentration was maintained below the Km value, the assay remained sensitive especially to competitive inhibitors, allowing reliable determination of IC_{50} values (Zhu et al., 2020). Reported Km values for SARS-CoV-2 3CLpro vary considerably depending on assay conditions, including enzyme concentration, substrate type, temperature, and buffer composition. Previous studies have reported Km values ranging from approximately 10 to 536 μM under different experimental settings (Belenkaya et al., 2023; Dražić et al., 2021; Samrat et al., 2022; Zhu et al., 2020). The Km value obtained in the present study (123.96 μM) falls within this reported range and is consistent with values determined under comparable assay conditions.

Screening and IC_{50} determination for the selected inhibitors

A FRET-based enzymatic assay was used to screen a commercial library of 384 structurally diverse natural compounds for SARS-CoV-2 3CLpro inhibition. Compounds were initially evaluated at a single concentration of 25 μM, consistent with previous 3CLpro screening studies (Kuzikov et al., 2021; Zhu et al., 2020). The distribution of normalized inhibition values is presented in Figure 2. Among the screened compounds, 57 exhibited more than 50% inhibition and were considered preliminary hits. After excluding intrinsically fluorescent compounds that could interfere with the assay, 24 candidates were selected for further evaluation based on inhibitory activity, predicted toxicity, assay compatibility, structural diversity, and literature relevance. For these, predicted toxicity data obtained from *in silico* toxicity analysis is given in Table S2.

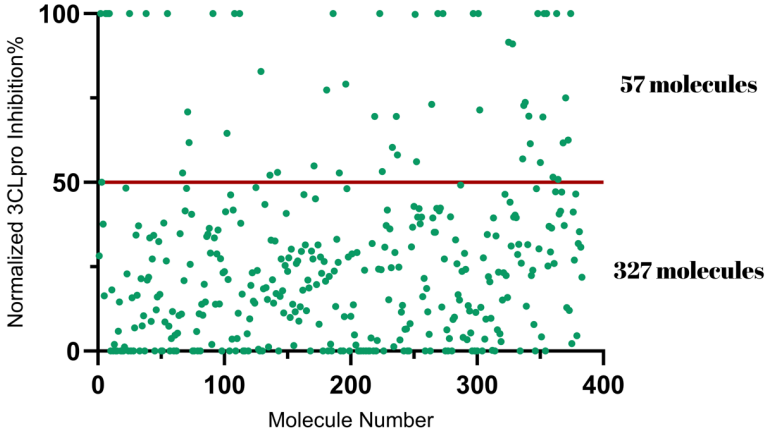

Figure 2. Distribution of normalized 3CLpro inhibition percentages for all 384 natural compounds

After selecting 24 compounds from the initial library of 384 natural products, their IC_{50} values were determined using seven inhibitor concentrations ranging from 0.1 μM to 100 μM, tested at constant enzyme and substrate concentrations. Among these, six compounds showed notably strong inhibitory activity, with IC_{50} values in the low concentration range (<55 μM), as listed in Table 1. From Table 1, it is also clear that most compounds exhibited relatively high IC_{50} values (>100 μM), reflecting moderate inhibition of 3CLpro, while a few such as Aloin B, Heterophyllin B, Artemitin, and Berberine Chloride showed low R^2 values in dose–response fitting, indicating weaker or inconsistent inhibition profiles, and these are provided in Figure S3. Detailed dose–response curves for the six most potent inhibitors are presented in Figure 3.

Table 1. Quantitative assessment of inhibitory potency and dose-response curve fitting reliability for 24 molecules

Molecule Name	IC_{50} (μM)	Molecule Name	IC_{50} (μM)	Molecule Name	IC_{50} (μM)
Vasicine	1.09	Chlorogenic acid	130.41	Orientin	>100
Palmitic acid	2.54	Levomefolic acid	316.28	Berberine Chloride	>100
Ginkgolic acid	11.23	EGCG	>100	Heterophyllin B	>100
Anacardic acid	11.60	EGCG Octaacetate	>100	Aloin B	>100
Fisetin	34.87	Neochlorogenic acid	299.03	(-) Hydrastine	>100
Neobavaisoflavone	54.41	Isochlorogenic acid B	>100	Berberine Chloride Hydrate	>100
Nobiletin[a]	< 10.00	(-)-Verbenone	>100	Resveratrol	>100
Rutin[b]	> 100.00	Narcissoside	>100	Artemitin	>100

[a] The initial dose–response curve for Nobiletin did not provide a reliable fit; however, its IC_{50} value (<10 μM) was subsequently confirmed using Dixon plot analysis (Figure S4.). Therefore, Nobiletin was included in the cytotoxicity and cell-based antiviral assays. [b] Although Rutin exhibited an IC_{50} value greater than 100 μM in the *in vitro* enzymatic assay, it was still included in cytotoxicity and antiviral testing because it is well known to be non-toxic to various cell types (El Gizawy et al., 2021; Mohd Abd Razak et al., 2023).

Among the six most potent natural compounds identified in this study, vasicine (IC_{50} = 1.09 μM) emerged as the strongest 3CLpro inhibitor. Vasicine is a quinazoline alkaloid known for broad pharmacological activity, and its fused aromatic structure enables hydrogen bonding and π–π interactions (Ghosh et al., 2021; Rudrapal et al., 2022). Docking studies have suggested interactions with several residues, including Arg131, Lys137, Thr199, and Leu288 (Salamat et al., 2024). To our knowledge, despite these computational predictions, no prior experimental evidence has demonstrated direct inhibition of SARS-CoV-2 3CLpro by vasicine. Our findings therefore provide the first biochemical evidence supporting vasicine as a direct 3CLpro inhibitor.

Palmitic acid (IC_{50} = 2.54 μM), a saturated fatty acid with essential metabolic functions, also demonstrated strong inhibition. Although palmitic acid is involved in viral protein palmitoylation and host inflammatory pathways, processes that may facilitate SARS-CoV-2 infection (Joshi, Jadeja, & Zhou, 2021; Kong, Li, Qian, & Xia, 2025), *in silico* studies suggested possible interactions near the catalytic pocket through hydrogen bonding and hydrophobic interactions (Kannan, Anandan, Srinivasan, & Vijayasingh, 2022; Khairan, 2021). On the other hand, our kinetic analysis demonstrated an uncompetitive inhibition mechanism, as explained later, indicating preferential binding to the enzyme–substrate complex under the present experimental conditions. The potent enzymatic inhibition observed here therefore suggests that the inhibitory mechanism may differ from that predicted solely by computational docking and supports further evaluation in cell-based systems.

Ginkgolic acid and anacardic acid, both characterized by a phenolic head group and long hydrophobic alkyl chain, also displayed notable 3CLpro inhibition. Their structural features support hydrogen bonding, π–π stacking, and extensive hydrophobic interactions with catalytic residues such as Cys145, His41, and Glu166 (Chen et al., 2021; Li et al., 2022). Although differences in alkyl-chain unsaturation may influence flexibility, particularly for ginkgolic acid, both compounds have been previously reported as dual 3CLpro/PLpro inhibitors with low-micromolar IC_{50} values, consistent with our findings (Chen et al., 2021; Li et al., 2022).

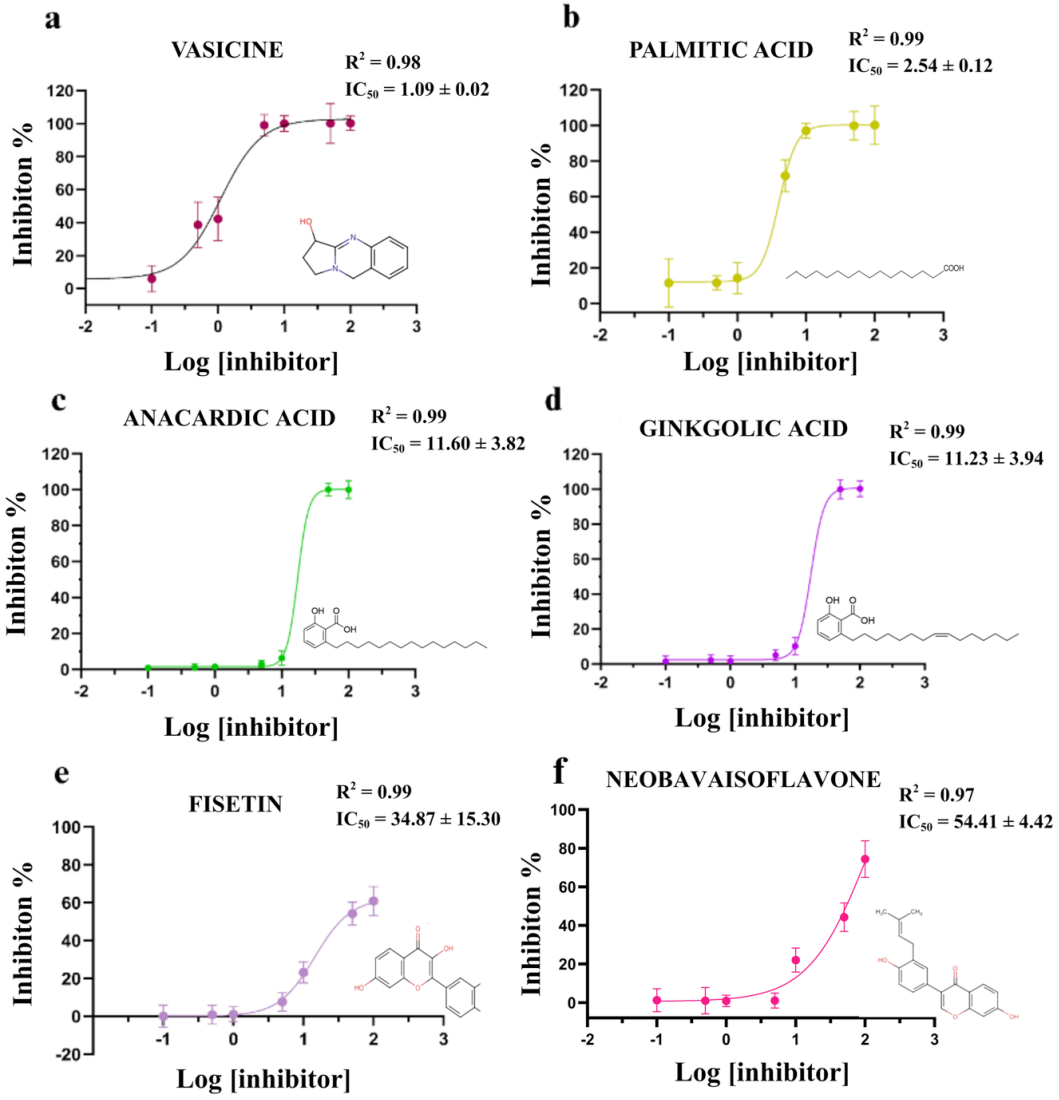

Figure 3. Dose-response curves of the six most potent inhibitors (a) Vasicine, (b) Palmitic acid, (c) Anacardic acid, (d) Ginkgolic acid, (e) Fisetin, and (f) Neobavaisoflavone.

Fisetin (IC_{50} = 34.87 μM), a flavonoid with antiviral and anti-inflammatory properties, interacts with viral enzymes through its hydroxylated aromatic scaffold, enabling hydrogen bonding and π–π interactions with residues such as Cys145, His41, and Glu166 (Chaves et al., 2022; Jamali et al., 2021). Prior studies have also shown potent antiviral activity in cell-based assays and potential modulation of host inflammatory responses supporting its relevance as a multi-target antiviral compound (Kolodnitsky, Ionov, Gravel, & Poroikov, 2023).

Neobavaisoflavone (IC_{50} = 54.41 μM), a prenylated isoflavonoid, has been highlighted in multiple computational studies for its favorable binding to 3CLpro and PLpro, mediated by hydrogen bonding and hydrophobic interactions with key catalytic residues (Magwaza et al., 2024; Verma et al., 2020). Although direct biochemical data have been limited, our experimental results support these predictions and indicate meaningful inhibition at higher concentration levels. In addition to these six lead inhibitors, two other compounds, Nobiletin and Rutin, were also selected for kinetic evaluation due to their relatively low IC_{50} values as well as established non-toxicity. Neochlorogenic Acid, Chlorogenic Acid, and Naringenin were also

subjected to preliminary concentration-dependent evaluation; however, their inhibition profiles did not permit reliable mechanistic fitting and were therefore excluded from further kinetic analysis.

Determination of inhibition kinetics and kinetic parameters for the selected compounds

To gain mechanistic insight into enzyme–inhibitor interactions beyond IC_{50} determination, the six most promising compounds were selected for steady-state kinetic analysis based on their inhibitory activity, dose–response profiles and predicted toxicity. The resulting Michaelis–Menten and Lineweaver–Burk plots are presented in Figure 4 and Figure 5.

Using GraphPad, Michaelis–Menten and Lineweaver–Burk plots obtained for Vasicine (Figure 4a and 4b, respectively), which is the most potent inhibitor, showed simultaneous changes in the apparent $K_{m,app}$ and $V_{max,app}$ values, indicating mixed-type inhibition of 3CLpro, with the best model fit at 100 nM enzyme concentration ($R^2 = 0.99$, Table S3). Vasicine exhibited a K_i value of 3.70 ± 3.80 μM and an αK_i of 47.95 μM (α = 12.95 ± 10.44), suggesting moderate binding to both the free enzyme and the enzyme–substrate complex. The increase in $K_{m,app}$ at higher inhibitor concentrations further implies interference with substrate binding, possibly through interactions at secondary binding sites that may contribute to substrate inhibition. Detailed kinetic parameters, including $K_{m,app}$ and $V_{max,app}$ values at different inhibitor concentrations, are provided in Table S4.

Kinetic analyses performed for Palmitic acid indicated that it acts as an uncompetitive inhibitor of 3CLpro. Figure 4c and 4d showed that increasing concentrations of palmitic acid led to a decrease in both $V_{max,app}$ and $K_{m,app}$ values, which is confirmed through nonlinear regression analysis, providing the best overall fit ($R^2 = 0.891$) for uncompetitive inhibition, as provided in Table S5. The kinetic parameters further supported this mechanism, where both $K_{m,app}$ and $V_{max,app}$ decreased proportionally across 1–50 μM inhibitor concentration, yielding a K_i of 8.03 ± 6.35 μM and αK_i of 5.60 μM (α = 0.69 ± 0.18), consistent with preferential binding to the enzyme–substrate complex. These results are also provided in Table S6.

Regarding Neobavaisoflavone, kinetic analyses indicated that it predominantly acts as a competitive inhibitor. Michaelis–Menten and Lineweaver–Burk plots (Figure 4e and 4f) showed that increasing inhibitor concentrations led to a rightward shift in the substrate–velocity curve without significantly affecting Vmax, a hallmark of competitive inhibition. Analysis performed using GraphPad confirmed this observation, with competitive inhibition providing the best overall fit ($R^2 = 0.941$), as presented in Table S7. The average K_i value was calculated as 19.61 ± 3.60 μM, and analysis yielded an αK_i value of 57.92 μM (α = 3.12 ± 1.76), further supporting a predominantly competitive inhibition mechanism. Although mild mixed-type behavior appeared at high concentrations, competitive binding was the primary mechanism. Detailed kinetic parameters are presented in Table S8.

Through nonlinear regression analysis performed for Fisetin (Table S9.), both mixed-type and non-competitive inhibition models fit the data with similarly high accuracy ($R^2 = 0.961$). However, detailed kinetic evaluation revealed that increasing fisetin concentrations led to an increase in $K_{m,app}$ and a decrease in $V_{max,app}$, a defining feature of mixed-type inhibition. This behavior indicates that fisetin can bind to both the free enzyme and the enzyme–substrate complex, affecting both substrate affinity and catalytic turnover. Fisetin displayed a K_i of 30.92 ± 1.83 μM, an αK_i of 105.92 μM, and an α value of 3.39 ± 1.10 (Table S10.). Although earlier studies reported a non-competitive inhibition for fisetin against SARS-CoV-2 Mpro based on assays where a single fixed inhibitor concentration and limited substrate ranges were used (Chaves et al., 2022), our detailed kinetic analysis across multiple inhibitor concentrations and an extended concentration range of substrate clearly supports a mixed-type inhibition mechanism. Although the antiviral potential of some of these natural compounds has been investigated previously, mostly in *in silico* docking studies, to the best of our knowledge, this is the first study characterizing the mechanism-of-inhibition of vasicine, palmitic acid and neobavaisoflavone against 3CLpro.

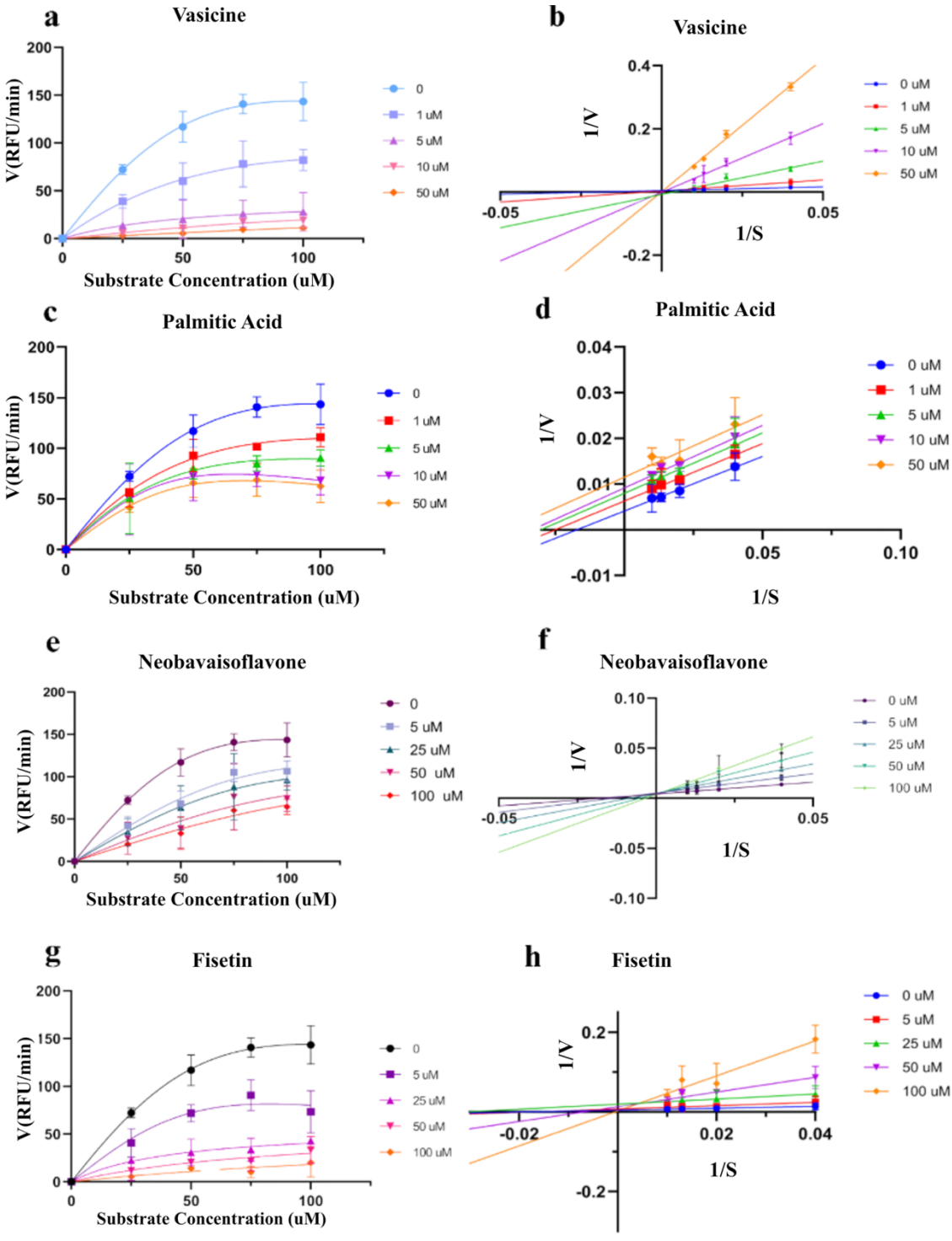

Figure 4. Michaelis–Menten and Lineweaver–Burk plots obtained for the most potent inhibitors at a fixed enzyme (100 nM) and varying substrate concentrations (a, b) Vasicine; (c, d) Palmitic Acid; (e, f) Neobavaisoflavone and (g, h) Fisetin.

The inhibition data for the remaining two most potent inhibitors, Ginkgolic acid and its analog Anacardic acid, revealed strong, concentration-dependent suppression of SARS-CoV-2 3CLpro activity, as shown in the Michaelis–Menten plots in Figure 5.

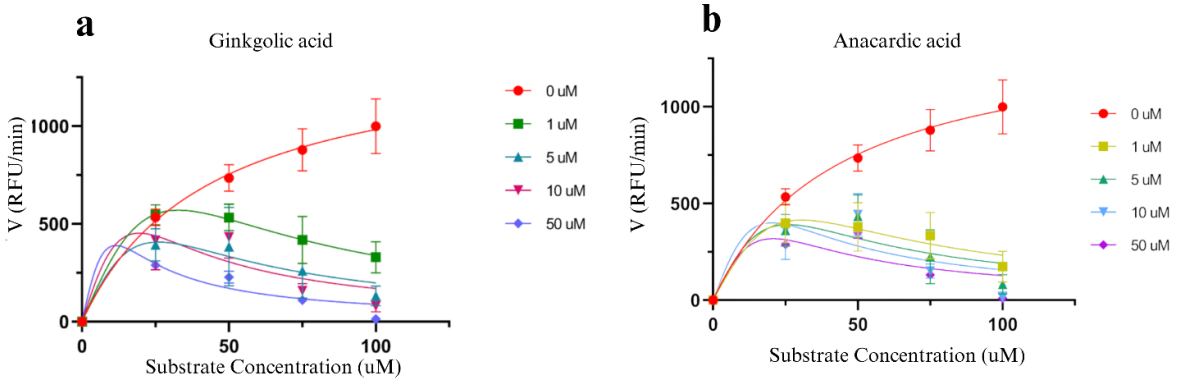

Figure 5. Michaelis–Menten plots obtained for (a) Ginkgolic acid and (b) Anacardic acid

At 100 nM enzyme concentration, enzymatic activity remained strongly suppressed across all substrate concentrations, and was further inactivated with increasing inhibitor concentrations, as shown in Figure 5a and 5b. Kinetic analyses performed for both Ginkgolic and Anacardic acids, as presented in Table S11 and S12, respectively, suggest substrate inhibition rather than the other reversible inhibition models (competitive, uncompetitive, or mixed type); however, the decreasing pattern observed in enzymatic activity in the presence of both inhibitors is also a characteristic of covalent (irreversible) inhibition, where the inhibitor forms a stable, permanent bond with a key catalytic residue, such as Cys145, leading to complete enzymatic inactivation. Therefore, inhibition mechanisms for both Ginkgolic and Anacardic acids may involve a dual inhibition mechanism, characterized primarily by substrate inhibition with potential contribution of covalent inhibition. Literature findings further strengthen these interpretations. Ginkgolic acid was reported to exhibit an IC_{50} of 1.79 ± 0.58 μM against SARS-CoV-2 3CLpro and to display time-dependent inhibition kinetics and irreversible inactivation in dilution recovery assays. Docking studies also indicate its binding near the catalytic cysteine residue, supporting the likelihood of covalent bond formation (Chen et al., 2021). Similarly, Anacardic acid was described as a covalent 3CLpro inhibitor with an IC_{50} of 2.07 ± 0.35 μM, showing irreversible inactivation and predicted interactions near the Cys145–His41 catalytic dyad (Chen et al., 2021). However, for anacardic acid, Li et al. reported a reversible mixed-type inhibition based on mass spectrometry evidence showing no covalent adduct formation (Li et al., 2022). In our study, the irreversible decline in enzyme activity over time and the strong fit to substrate inhibition models suggest that both substrate-driven suppression and covalent-like irreversible inactivation may occur. This dual mechanism reconciles conflicting reports in the literature and aligns with our kinetic findings, suggesting that both ginkgolic and anacardic acids exhibit notable inhibitory activity through a combination of substrate inhibition and irreversible enzyme inactivation, although their mechanisms may involve both specific and nonspecific processes and therefore require further validation.

As mentioned earlier, we also performed dose-dependent inhibition assays for two additional compounds, Nobiletin and Rutin, at a fixed enzyme and substrate concentrations. Through Dixon plot analysis (Figure S2.), their K_i values were determined, and the resulting inhibition kinetic parameters together with those obtained for the 6 most-potent inhibitors are summarized in Table 2 for clarity.

Table 2. Summary of inhibition kinetic parameters for the eight selected compounds

Molecule name	K_i (μM)	α	Inhibition Type	R^2
Vasicine	3.70 ± 3.80	12.95 ± 10.44	Mixed Type	0.99
Palmitic acid	8.03 ± 6.35	0.69 ± 0.18	Uncompetitive	0.89
Neobavaisoflavone	19.61 ± 3.60	3.12 ± 1.76	Competitive	0.94
Fisetin	30.92 ± 1.83	3.39 ± 1.00	Mixed Type	0.96
Ginkgolic acid			Covalent (Irreversible)[a]	
Anacardic acid			Covalent (Irreversible)[a]	
Nobiletin[b]	102.70 ± 0.08	ND[c]	ND	0.98
Rutin[b]	210.42 ± 0.01	ND	ND	0.98

[a] As classical reversible inhibition kinetic parameters are not applicable to covalent type inhibition, Ki values for covalent inhibitors cannot be obtained. [b] Ki values for Nobiletin and Rutin were derived from Dixon plot analysis (Figure S4.). [c] ND: Not determined.

Based on the enzymatic screening results, kinetic modeling, and IC_{50} profiles, these eight compounds were further evaluated through cell-based assays. Their strong enzymatic performance and pharmacological relevance justified prioritizing them for cytotoxicity (CC_{50}) and antiviral efficacy (EC_{50}) testing in Vero E6 cells to assess their therapeutic potential.

Assessment of *in vitro* cytotoxicity and antiviral efficacy for the selected compounds

The cytotoxicity of the eight selected compounds was assessed in Vero E6 cells using the MTT assay following 24 and 48 h of exposure at concentrations ranging from 0.78 to 25 μM. Cell viability was expressed relative to untreated controls, and compounds reducing viability below 70% were classified as cytotoxic. The resulting dose- and time-dependent cytotoxicity profiles are shown in Figure 6. From Figure 6, the cytotoxicity profiles of the tested compounds differed markedly between 24 and 48 h of exposure. After 24 h, all compounds except palmitic acid maintained cell viability above 70% at concentrations ≤ 3.125 μM. Fisetin and palmitic acid exhibited early cytotoxicity at concentrations ≥6.25 μM, whereas prolonged exposure (48 h) increased the cytotoxicity of ginkgolic acid, anacardic acid, neobavaisoflavone, vasicine, and nobiletin at concentrations above 6.25 μM. Among the tested compounds, rutin consistently maintained cell viability above 70% even at 25 μM, confirming its non-toxic nature.

The cytotoxicity profiles of anacardic acid, ginkgolic acid, and rutin were consistent with previous reports (Chen et al., 2021; El Gizawy et al., 2021; Lin et al., 2012; Mohd Abd Razak et al., 2023). In contrast, no previous cytotoxicity data in Vero E6 cells were identified for neobavaisoflavone, vasicine, or nobiletin, while fisetin exhibited cytotoxicity at lower concentrations than previously reported, possibly due to differences in experimental conditions (Chaves et al., 2022; Zandi et al., 2011).

Palmitic acid showed the greatest cytotoxicity among the tested compounds. This effect is consistent with previous studies demonstrating that excess palmitic acid induces mitochondrial dysfunction, oxidative stress, and endoplasmic reticulum stress, ultimately promoting apoptotic cell death (Demirel & Batırel, 2018; Korbecki & Bajdak-Rusinek, 2019).

Based on the cytotoxicity results, 2.5 μM was selected as the highest non-cytotoxic concentration for antiviral evaluation in SARS-CoV-2-infected Vero E6 cells. To further assess concentration-dependent effects, additional experiments were performed at 1.25, 2.5, 5.0, and 10.0 μM, and the results are presented in

Figure S5. Figure 7 shows the fold change in SARS-CoV-2 genomic RNA levels relative to the housekeeping gene (HKG) following treatment with compounds C1–C8 at 2.5 µM. At 24 h post-infection, palmitic acid (C4), vasicine (C5), and anacardic acid (C6) produced the greatest reductions in viral RNA levels. By 72 h, rutin (C3), palmitic acid (C4), and vasicine (C5) exhibited more pronounced antiviral effects, whereas the activity of anacardic acid (C6) diminished over time, resulting in increased viral RNA levels. CPE was also monitored microscopically during the antiviral experiments; however, no clear reduction in virus-induced cytopathic changes was observed in the compound-treated groups compared with the untreated virus control. Therefore, antiviral effects were primarily evaluated using the more quantitative RT-qPCR-based viral RNA measurements.

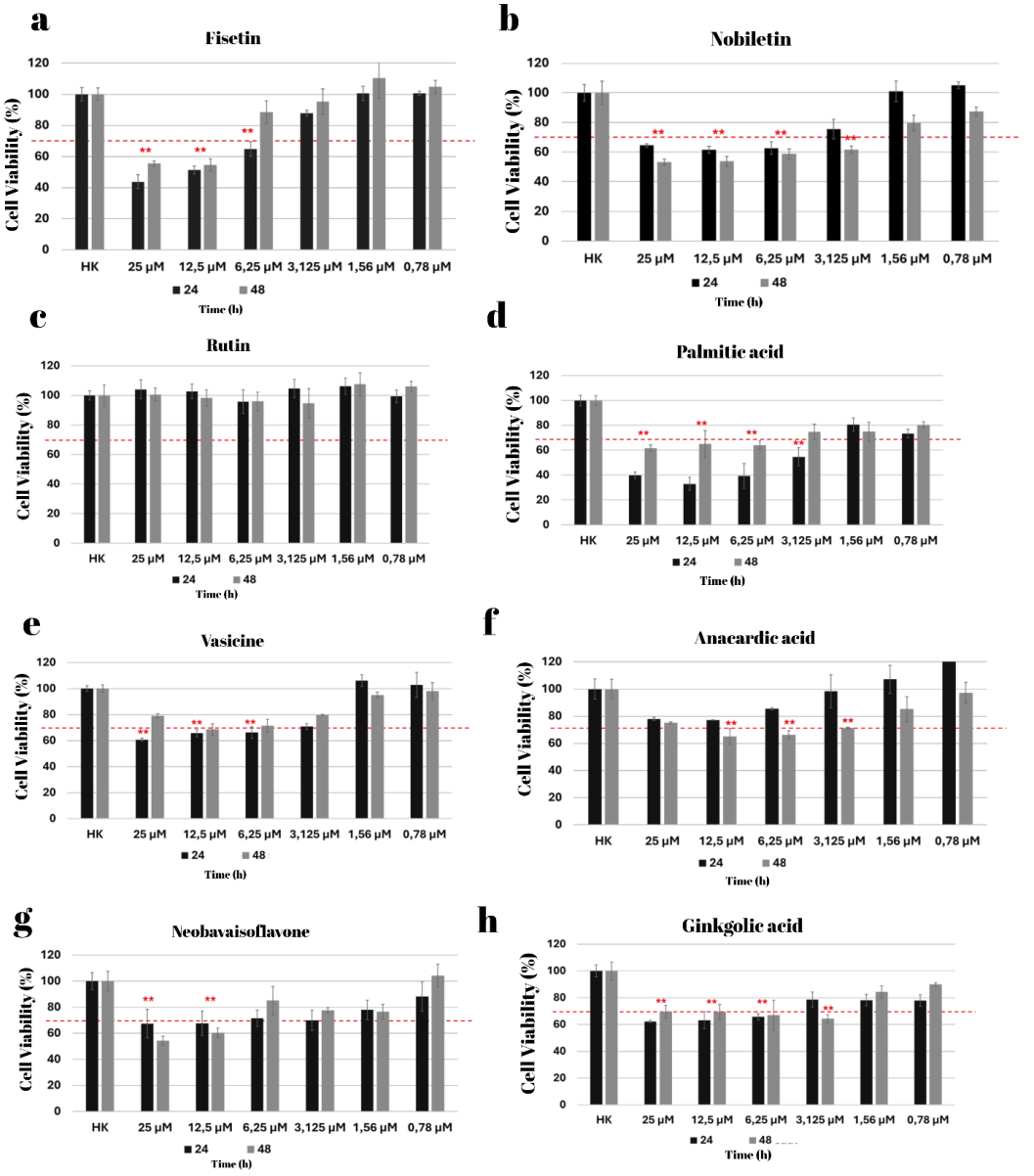

Figure 6. Evaluation of cytotoxic effects of the selected natural compounds on Vero cells at 24 and 48 hours (a) Fisetin, (b) Nobiletin, (c) Rutin, (d) Palmitic acid, (e) Vasicine, (f) Anacardic Acid, (g) Neobavaisoflavone, and (h) Ginkgolic Acid

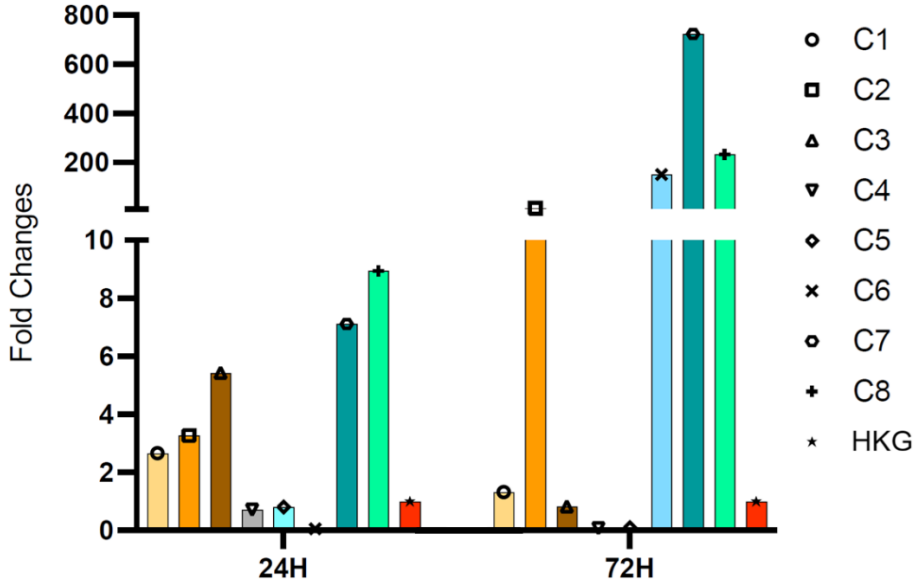

Figure 7. Fold change levels of SARS-CoV-2 in Vero cells treated with compounds (C1–C8, at 2.5 μM) at 24 h and 72 h post-inoculation. C1: Fisetin, C2: Nobiletin, C3: Rutin, C4: Palmitic Acid, C5: Vasicine, C6: Anacardic Acid, C7: Neobavaisoflavone, C8: Ginkgolic Acid, and HKG: Housekeeping gene

Previous studies have demonstrated the antiviral activities of anacardic acid, ginkgolic acid, and fisetin using authentic SARS-CoV-2 infection models, reporting low-micromolar EC_{50} values under non-cytotoxic conditions (Chaves et al., 2022; Chen et al., 2021). However, these studies primarily employed plaque reduction assays, whereas the present study evaluated antiviral responses by RT-qPCR-based quantification of viral genomic RNA together with cytopathic effect observations. Differences between the antiviral profiles observed here and those reported previously are therefore likely attributable to differences in assay methodology and endpoint sensitivity rather than intrinsic antiviral activity.

Although the antiviral effects observed in this study were generally moderate, clear compound-specific and time-dependent differences were identified under standardized experimental conditions. In particular, this work provides comparative antiviral data for several natural compounds, including vasicine, palmitic acid, neobavaisoflavone, rutin, and nobiletin, for which cell-based antiviral evidence remains limited. By integrating enzymatic inhibition, cytotoxicity, and RT-qPCR-based antiviral evaluation within a single experimental workflow, the present study provides a comprehensive experimental dataset for future investigation of natural SARS-CoV-2 3CLpro inhibitors.

Further discussion and future directions

Although the FRET-based assay used in this study provides a rapid and sensitive approach for identifying SARS-CoV-2 3CLpro inhibitors, fluorescence-based enzymatic assays may be susceptible to artifacts such as colloidal aggregation, redox activity, covalent modification, or fluorescence interference, particularly when evaluating natural products (Ma, Tan, Choza, Wang, & Wang, 2022; O'Donnell, Tummino, Bardine, Craik, & Shoichet, 2021). Therefore, fluorescence interference was monitored using compound-only control wells, and inhibitory activity was confirmed through dose–response experiments and steady-state kinetic analysis rather than single-point measurements. In

addition, the assay buffer contained EDTA and DTT to minimize metal-dependent and redox-related interference. Selected enzymatic hits were subsequently evaluated in SARS-CoV-2-infected Vero E6 cells, providing additional biological validation that supports the functional relevance of the identified inhibitors. It should be noted that the recombinant 3CLpro used in this study contained an N-terminal MBP tag. Although the construct displayed robust catalytic activity and its performance was validated using GC376 as a positive control, the presence of the MBP tag may influence the apparent kinetic parameters relative to those obtained with the untagged protease.

Particular caution is warranted for compounds such as ginkgolic acid and anacardic acid, whose long hydrophobic alkyl chains and reactive functional groups have been associated with aggregation-based or nonspecific inhibition. Although these compounds showed potent inhibitory activity, additional studies are required to confirm their selectivity and mechanism of action.

Future work should include detergent-based aggregation controls, enzyme dilution assays, and fluorescence-independent validation methods to distinguish specific inhibitors from assay artifacts (O'Donnell et al., 2021; Ye et al., 2024). Structural approaches, including molecular docking or complementary biophysical studies, would further clarify inhibitor binding modes, while counter-screening against related cysteine proteases would help evaluate selectivity and potential off-target effects.

Overall, this study provides a comprehensive experimental dataset integrating enzymatic screening, kinetic characterization, and cell-based antiviral evaluation of natural SARS-CoV-2 3CLpro inhibitors. Additional biochemical and structural studies will further strengthen the therapeutic potential of the identified compounds.

CONCLUSION

In this study, a comprehensive and multi-stage experimental workflow was established to evaluate the antiviral potential of natural compounds targeting the SARS-CoV-2 3CLprotease. Initially, a commercially available library of 384 natural compounds was screened through a high-throughput FRET-based enzymatic assay, providing a comprehensive experimental dataset for natural 3CLpro inhibitors. Based on the screening outcomes, 24 compounds exhibiting notable inhibitory activity were selected for dose–response studies, from which six lead molecules were further analyzed in detailed enzyme kinetic experiments to determine their modes of inhibition and K_i values. This kinetic investigation of natural 3CLpro inhibitors represents one of the few studies combining systematic screening with detailed kinetic characterization of multiple natural inhibitors. Subsequently, these lead compounds were tested in SARS-CoV-2-infected Vero E6 cells, where cytotoxicity and RT-qPCR-based viral load analyses confirmed their biological relevance. Together, these findings support a relationship between *in vitro* enzymatic inhibition and cell-based antiviral activity.

ACKNOWLEDGEMENTS

This research was supported by the Scientific and Technological Research Council of Turkiye (TUBITAK) under Grant No. 121C133.

AUTHOR CONTRIBUTION STATEMENT

Writing-Original Draft, Formal analysis, Data curation (BTB); Methodology, Investigation, Supervision (OB), Formal analysis, Data curation (IEK); Validation, Supervision (AS); Formal analysis, Data curation, Methodology, Investigation (AO); Conceptualization, Writing-Review & editing, Methodology, Project administration, Funding acquisition (DY).

CONFLICT OF INTEREST

The authors declare that there is no conflict of interest.

REFERENCES

Atanasov, A. G., Zotchev, S. B., Dirsch, V. M., Orhan, I. E., Banach, M., Rollinger, J. M.,…Supuran, C. T. (2021). Natural products in drug discovery: advances and opportunities. *Nature Reviews Drug Discovery*, *20*(3), 200–216. https://doi.org/10.1038/s41573-020-00114-z

Bahun, M., Jukić, M., Oblak, D., Kranjc, L., Bajc, G., Butala, M.,…Poklar Ulrih, N. (2022). Inhibition of the SARS-CoV-2 3CLpro main protease by plant polyphenols. *Food Chemistry*, *373*. https://doi.org/10.1016/j.foodchem.2021.131594

Belenkaya, S. V., Merkuleva, I. A., Yarovaya, O. I., Chirkova, V. Y., Sharlaeva, E. A., Shanshin, D. V.,…Shcherbakov, D. N. (2023). The main protease 3CLpro of the SARS-CoV-2 virus: how to turn an enemy into a helper. *Frontiers in Bioengineering and Biotechnology*, *11*. https://doi.org/10.3389/fbioe.2023.1187761

Chaves, O. A., Fintelman-Rodrigues, N., Wang, X., Sacramento, C. Q., Temerozo, J. R., Ferreira, A. C.,…Souza, T. M. L. (2022). Commercially Available Flavonols Are Better SARS-CoV-2 Inhibitors Than Isoflavone and Flavones. *Viruses*, *14*(7). https://doi.org/10.3390/v14071458

Chen, Z., Cui, Q., Cooper, L., Zhang, P., Lee, H., Chen, Z.,…Du, R. (2021). Ginkgolic acid and anacardic acid are specific covalent inhibitors of SARS-CoV-2 cysteine proteases. *Cell Bioscience*, *11*, 45. https://doi.org/10.1186/s13578-021-00564-x.

Coelho, C., Gallo, G., Campos, C. B., Hardy, L., & Wurtele, M. (2020). Biochemical screening for SARS-CoV-2 main protease inhibitors. *PLoS ONE*, *15*(10). https://doi.org/10.1371/journal.pone.0240079

Demirel, T., & Batirel, S. (2018). Palmitic acid induces endoplasmic reticulum stress in AML12 liver cells. *Marmara Medical Journal*, *31*(1), 40–46. https://doi.org/10.5472/marumj.362169

Dražić, T., Kühl, N., Leuthold, M. M., Behnam, M. A. M., & Klein, C. D. (2021). Efficiency Improvements and Discovery of New Substrates for a SARS-CoV-2 Main Protease FRET Assay. *SLAS Discovery*, *26*(9), 1189–1199. https://doi.org/10.1177/24725552211020681

El Gizawy, H. A., Boshra, S. A., Mostafa, A., Mahmoud, S. H., Ismail, M. I., Alsfouk, A. A.,… Al-Karmalawy, A. A. (2021). Pimenta dioica (L.) merr. bioactive constituents exert anti-sars-cov-2 and anti-inflammatory activities: Molecular docking and dynamics, in-vitro, and in vivo studies. *Molecules*, *26*(19). https://doi.org/10.3390/molecules26195844

Ferreira, J.C., Fadl, S., Ilter, M., Pekel, H., Rezgui, R., Sensoy, O., & Rabeh., W.M., (2021) Dimethyl sulfoxide reduces the stability but enhances catalytic activity of the main SARS-CoV-2 protease 3CLpro, *The FASEB Journal*, *35*, e21774.

Ghosh, R., Chakraborty, A., Biswas, A., & Chowdhuri, S. (2021). Identification of alkaloids from Justicia adhatoda as potent SARS CoV-2 main protease inhibitors: An in-silico perspective. *Journal of Molecular Structure*, *1229*. https://doi.org/10.1016/j.molstruc.2020.129489

Glaab, E., Manoharan, G. B., & Abankwa, D. (2021). Pharmacophore Model for SARS-CoV-2 3CLpro Small-Molecule Inhibitors and in-Vitro Experimental Validation of Computationally Screened Inhibitors. *Journal of Chemical Information and Modeling*, *61*(8), 4082–4096. https://doi.org/10.1021/acs.jcim.1c00258

Hariono, M., Hariyono, P., Dwiastuti, R., Setyani, W., Yusuf, M., Salin, N., & Wahab, H. (2021). Potential SARS-CoV-2 3CLpro inhibitors from chromene, flavonoid and hydroxamic acid compound based on FRET assay, docking and pharmacophore studies. *Results in Chemistry*, *3*. https://doi.org/10.1016/j.rechem.2021.100195

Isidoro, C., Chiung-Fang Chang, A., & Sheen, L. Y. (2022). Natural products as a source of novel drugs for treating SARS-CoV2 infection. *Journal of Traditional and Complementary Medicine, 12*(1), 1–5. https://doi.org/10.1016/j.jtcme.2022.02.001

Jamali, N., Soureshjani, E. H., Mobini, G. R., Samare-Najaf, M., Clark, C. C. T., & Saffari-Chaleshtori, J. (2021). Medicinal plant compounds as promising inhibitors of coronavirus (COVID-19) main protease: an in-silico study. *Journal of Biomolecular Structure and Dynamics*, *40*(17), 8073–8084. https://doi.org/10.1080/07391102.2021.1906749

Joshi, C., Jadeja, V., & Zhou, H. (2021). Molecular mechanisms of palmitic acid augmentation in covid-19 pathologies. *International Journal of Molecular Sciences*, *22*(13). https://doi.org/10.3390/ijms22137127

Kannan, V., Anandan, R., Srinivasan, S., Vijayasingh, N., Lavana, S., Singaravelud, U. & Athiappan, M. (2022). Metabolites of Docosahexaenoic Acid Produced by Probiotic Bacillus cereus able to Inhibit 2BX4 and 6LU7 Receptors of SARS-COV-2. *Advances in Bioresearch*, *13*(5), 183-214. doi: 10.15515/abr.0976-4585.13.5.183214

Khairan, K., Idroes, R., Tumilaar, S. G., Tallei, T. E., Idroes, G. M., Rahmadhany, F.,…Earlia, N. (2021). Molecular docking study of fatty acids from Pliek U Oil in the inhibition of SARS-CoV-2 protein and enzymes. *IOP Conference Series: Materials Science and Engineering*, *1087*(1), 012058. https://doi.org/10.1088/1757-899x/1087/1/012058

Khamto, N., Boontawee, P., Choommongkol, V., Pruksaphon, K., Patnin, S., Suree, N.,...Meepowpan, P. (2025). Discovery of Galloyl–Flavonoid Conjugates as SARS-CoV-2 3CLpro Inhibitors: Understanding Binding Interactions Through Computational Approaches. *International Journal of Molecular Sciences*, *26*(19), 9742.

Kolodnitsky, A., Ionov, N., Gravel, I., & Poroikov, V. (2023). Natural compounds from medicinal plants against COVID-19. *Exploration of Drug Science*, *1*, 253–275. https://doi.org/10.37349/eds.2023.00017

Kong, C., Li, Y., Qian, Y., & Xia, P. (2025). Palmitic acid esters of hydroxy stearic acid suppresses SARS-CoV-2 infection through inhibiting the non-canonical inflammasome. *HLife*, *3*(9), 452-454. https://doi.org/10.1016/j.hlife.2025.01.005

Korbecki, J., & Bajdak-Rusinek, K. (2019). The effect of palmitic acid on inflammatory response in macrophages: an overview of molecular mechanisms. *Inflammation Research*, 68(11), 915–932. https://doi.org/10.1007/s00011-019-01273-5

Krüger, N., Kronenberger, T., Xie, H., Rocha, C., Pöhlmann, S., Su, H.,…Pillaiyar, T. (2023). Discovery of Polyphenolic Natural Products as SARS-CoV-2 Mpro Inhibitors for COVID-19. *Pharmaceuticals*, *16*(2). https://doi.org/10.3390/ph16020190

Kuzikov, M., Costanzi, E., Reinshagen, J., Esposito, F., Vangeel, L., Wolf, M.,… Zaliani, A. (2021). Identification of Inhibitors of SARS-CoV-2 3CL-Pro Enzymatic Activity Using a Small Molecule in-Vitro Repurposing Screen. *ACS Pharmacology and Translational Science*, *4*(3), 1096–1110. https://doi.org/10.1021/acsptsci.0c00216

Li, D., Yan, G., Zhou, W., Si, S., Liu, X., Zhang, J.,... Chen, Y. (2022). Ginkgolic acid and anacardic acid are reversible inhibitors of SARS-CoV-2 3-chymotrypsin-like protease. *Cell & Bioscience*, *12*(1), 65.

Lin, Y. J., Chang, Y. C., Hsiao, N. W., Hsieh, J. L., Wang, C. Y., Kung, S. H.,…Lin, C. W. (2012). Fisetin and rutin as 3C protease inhibitors of enterovirus A71. *Journal of Virological Methods*, *182*(1–2), 93–98. https://doi.org/10.1016/j.jviromet.2012.03.020

Ma, C., Tan, H., Choza, J., Wang, Y., & Wang, J. (2022). Validation and invalidation of SARS-CoV-2 main protease inhibitors using the Flip-GFP and Protease-Glo luciferase assays. *Acta Pharmaceutica Sinica B*, *12*(4), 1636-1651, https://doi.org/10.1016/j.apsb.2021.10.026.

Magwaza, N. N., Mushebenge, A. G. A., Ugbaja, S. C., Mbatha, N. A., Khan, R. B., & Kumalo, H. M. (2024). Mechanistic Insights into Targeting SARS-CoV-2 Papain-like Protease in the Evolution and Management of COVID-19. *BioChem*, *4*(3), 268–299. https://doi.org/10.3390/biochem4030014

Malone, B., Urakova, N., Snijder, E. J., & Campbell, E. A. (2022). Structures and functions of coronavirus replication–transcription complexes and their relevance for SARS-CoV-2 drug design. *Nature Reviews Molecular Cell Biology*, *23*(1), 21–39. https://doi.org/10.1038/s41580-021-00432-z

Mohd Abd Razak M.R., Jelas N.H., Muhammad A., Padlan N., Sa'at, M.N.F., Azizan M.A.,…Mohamed, A.F.S. (2023) In-Vitro Anti-SARS-CoV-2 Activities of Curcumin and Selected Phenolic Compounds, *Natural Product Communications*, *18*(9): 1–9. https://doi.org/10.1177/1934578X231188861

Nguyen, T. T. H., Jung, J. H., Kim, M. K., Lim, S., Choi, J. M., Chung, B.,…Kim, D. (2021) The inhibitory effects of plant derivate polyphenols on the main protease of SARS coronavirus 2 and their structure–activity relationship. *Molecules*, *26*(7).

O'Donnell, H.R., Tummino, T.A., Bardine, C., Craik, C.S., & Shoichet, B.K., (2021). Colloidal Aggregators in Biochemical SARS-CoV-2 Repurposing Screens. *Journal of Medicinal Chemistry*, *64*, 17530–17539.

Rudrapal, M., Gogoi, N., Chetia, D., Khan, J., Banwas, S., Alshehri, B.,…Walode, S. G. (2022). Repurposing of phytomedicine-derived bioactive compounds with promising anti-SARS-CoV-2 potential: Molecular docking, MD simulation and drug-likeness/ADMET studies. *Saudi Journal of Biological Sciences*, *29*(4), 2432–2446. https://doi.org/10.1016/j.sjbs.2021.12.018

Salamat, A., Kosar, N., Mohyuddin, A., Imran, M., Zahid, M. N., & Mahmood, T. (2024). SAR, molecular docking and molecular dynamic simulation of natural inhibitors against SARS-CoV-2 Mpro Spike Protein. *Molecules*, *29*(5), 1144.

Samrat, S. K., Xu, J., Xie, X., Gianti, E., Chen, H., Zou, J.,…Li, H. (2022). Allosteric inhibitors of the main protease of SARS-CoV-2. *Antiviral Research*, *205*. https://doi.org/10.1016/j.antiviral.2022.105381

Shen, Z., Ratia, K., Cooper, L., Kong, D., Lee, H., Kwon, Y.,…Xiong, R. (2022). Design of SARS-CoV-2 PLpro Inhibitors for COVID-19 Antiviral Therapy Leveraging Binding Cooperativity. *Journal of Medicinal Chemistry*, *65*(4), 2940–2955. https://doi.org/10.1021/acs.jmedchem.1c01307

Szabó, D., Crowe, A., Mamotte, C., & Strappe, P. (2024). Natural products as a source of Coronavirus entry inhibitors. *Frontiers in Cellular and Infection Microbiology*, *14*. https://doi.org/10.3389/fcimb.2024.1353971

Verma, S., Twilley, D., Esmear, T., Oosthuizen, C. B., Reid, A. M., Nel, M., & Lall, N. (2020). Anti-SARS-CoV Natural Products With the Potential to Inhibit SARS-CoV-2 (COVID-19). *Frontiers in Pharmacology*, *11*. https://doi.org/10.3389/fphar.2020.561334

World Health Organization (WHO). (2026). *COVID-19 deaths dashboard*. Retrieved from https://data.who.int/dashboards/covid19/deaths

Yadav, R., Chaudhary, J. K., Jain, N., Chaudhary, P. K., Khanra, S., Dhamija, P.,…Handu, S. (2021). Role of Structural and Non-Structural Proteins and Therapeutic Targets of SARS-CoV-2 for COVID-19. *Cells, 10*, 821. https://doi.org/10.3390/cells

Yang, Y., Zhang, F., Liu, S., Jin, W., Shao, Q., Li, C., & Fan, B. (2024). A study of the protease inhibitory activity component of SARS-CoV-2 3CL in Bletilla striata. *Frontiers in Natural Products*, *3*, 1372623.

Ye, J, Xu T, Zhang R, Liu X, Zhang C, & Chen Y. (2024). Invalidating betulinic acid as a potential inhibitor against the main protease of SARS-CoV-2 via combined approaches. *Steroids*, *212*, 109522. https://doi: 10.1016/j.steroids.2024.109522.

Zandi, K., Teoh, B. T., Sam, S. S., Wong, P. F., Mustafa, M. R., & AbuBakar, S. (2011). In-vitro antiviral activity of fisetin, rutin and naringenin against dengue virus type-2. *Journal of Medicinal Plants Research*, *5*(23), 5534-5539.

Zhu, W., Xu, M., Chen, C. Z., Guo, H., Shen, M., Hu, X.,…Zheng, W. (2020). Identification of SARS-CoV-2 3CL Protease Inhibitors by a Quantitative High-throughput Screening. *ACS Pharmacol. Transl. Sci*, *3*(5), 1008–1016. https://doi.org/10.1021/acsptsci.0c00108

Zong, K., Wei, C., Li, W., Ruan, J., Zhang, S., Li, J.,... Li, X. (2024). Identification of novel SARS-CoV-2 3CLpro inhibitors by molecular docking, in-vitro assays, molecular dynamics simulations and DFT analyses. *Frontiers in Pharmacology*, *15*, 1494953.